

Effect of temperature on concentrated electrolytes for advanced lithium ion batteries

Cite as: J. Chem. Phys. 154, 214503 (2021); doi: 10.1063/5.0049259

Submitted: 3 March 2021 • Accepted: 17 May 2021 •

Published Online: 2 June 2021



View Online



Export Citation



CrossMark

Mahesh Mynam,^{a)}  Surbhi Kumari, Bharath Ravikumar,  and Beena Rai 

AFFILIATIONS

TCS Research, Tata Research Development and Design Centre, 54B, Hadapsar Industrial Estate, Pune 411013, India

^{a)} Author to whom correspondence should be addressed: mahesh.mynam@tcs.com

ABSTRACT

Salt-concentrated electrolytes are emerging as promising electrolytes for advanced lithium ion batteries (LIBs) that can offer high energy density and improved cycle life. To further improve these electrolytes, it is essential to understand their inherent behavior at various operating conditions of LIBs. Molecular dynamics (MD) simulations are extensively used to study various properties of electrolytes and explain the associated molecular-level phenomena. In this study, we use classical MD simulations to probe the properties of the concentrated electrolyte solution of 3 mol/kg lithium hexafluorophosphate (LiPF₆) salt in the propylene carbonate solvent at various temperatures ranging from 298 to 378 K. Our results reveal that the properties such as ionic diffusivity and molar conductivity of a concentrated electrolyte are more sensitive to temperature compared to that of dilute electrolytes. The residence time analysis shows that temperature affects the Li⁺ ion solvation shell dynamics significantly. The effect of temperature on the transport and dynamic properties needs to be accounted carefully while designing better thermal management systems for batteries made with concentrated electrolytes to garner the advantages of these electrolytes.

Published under an exclusive license by AIP Publishing. <https://doi.org/10.1063/5.0049259>

I. INTRODUCTION

Lithium ion batteries (LIBs) continue to dominate the market of portable electronic devices since their commercialization three decades ago.¹ The high energy density and long cycle life of LIBs make them an indispensable part of modern society. LIBs are now emerging as energy storage systems for electric vehicles²⁻³ and electric grids integrated with renewable energy sources (e.g., solar energy),⁴ thus contributing toward a sustainable energy ecosystem. The increase in demand for batteries of higher energy density and enhanced cycle life calls for the research and development of novel methodologies and chemistries that enable advanced LIBs and beyond lithium ion battery technologies.

Despite their garnered success, LIBs are susceptible to certain safety issues such as short circuits,^{5,6} release of flammable and toxic gases,^{7,8} and thermal runaway of batteries.⁹⁻¹³ It can be attributed to overheating and overcharging of the batteries and highly volatile nature of the electrolyte.¹⁴ The side reactions between the electrolyte and the electrodes result in consumption of active materials, which in turn leads to the capacity fade of the battery.^{15,16} Commercial LIBs, typically, use an electrolyte of 1M solution of lithium-hexafluorophosphate (LiPF₆) salt in a mixture of cyclic

and linear polar organic solvents such as ethylene carbonate (EC), dimethyl carbonate (DMC), and ethyl methyl carbonate (EMC).¹⁷⁻¹⁹ The salt concentration (i.e., 1M) and composition of the solvent mixture (i.e., proportion of solvent and co-solvents) in the conventional electrolytes are chosen to maximize the ionic conductivity, which defines the power performance of the battery.^{20,21} Though the EC-based electrolytes offer higher ionic conductivity (11–15 mS/cm) and wide potential window (3–4.5 V), most of the issues faced by current generation LIBs are attributed to the electrolyte.^{14,20} Concerned with this, researchers worldwide are endeavoring to develop novel electrolyte materials that can address various issues associated with EC based electrolytes. For instance, room temperature ionic liquids (RTILs),²² solid-state inorganic electrolytes,²³ polymer electrolytes,²⁴ aqueous electrolytes,²⁵ and salt-concentrated organic electrolytes²⁶ are being proposed as alternatives to the conventional 1M organic carbonate-based electrolytes.

In recent years, owing to their ability to offer better thermal and reactive stabilities, the concentrated electrolytes are widely tested in the LIBs.^{27,28} These electrolytes have been shown to enable the formation of a stable and uniform solid-electrolyte-interface (SEI), resulting in long cycle life of batteries. For example, the LIB made

of the concentrated propylene carbonate (PC) based electrolyte (2.5 mol/kg LiPF₆ salt in PC) is shown to offer better cycling performance.²⁹ Besides offering better cycle life, the concentrated electrolytes have less corrosion of Al current collectors even at high potentials.^{30,31} Several studies highlight fast charging and enhanced charge/discharge cycles of batteries that use super-concentrated Li electrolytes of organic solvents.^{32,33} The concentrated electrolytes are also proposed to be potential candidates for high energy density Li-metal (Li–O₂ and Li–S) batteries. It was shown that Li-salt concentrated electrolytes enable better cycling^{34–36} with increased Coulombic efficiency and reduce the formation of dendrites that result in short-circuits³⁷ and other safety issues with Li metal batteries.^{29–31,38–40} In spite of these advantages, the application of the concentrated electrolytes is limited by their lower ionic conductivity and higher viscosity.⁴¹ The ionic conductivity of electrolyte impacts the internal resistance and rate capability of batteries.^{31,41,42} Identification of co-solvents that reduce the overall viscosity of the electrolyte and novel solvents offering various required properties that help reaping the benefits of the concentrated electrolytes is an active research today.

The improved cycling performance shown by the LIBs made of concentrated PC based electrolytes^{40,43–45} leads to renewed interest in the PC as the electrolytic solvent. Owing to its properties such as high dielectric constant ($\epsilon \approx 65$),⁴⁶ wide operating temperature limit (MP: -49°C , BP: 240°C), and wide electrochemical stability window, PC was the preferred choice of solvent in the first generation LIBs.⁴⁷ However, co-intercalation of PC along with Li⁺ ions into the graphite electrode and consequent disruption of the electrode led to poor cycle life of the batteries.^{47,48} The increased reduction of the anion and alleviation of solvent co-intercalation lead to better cycle life of batteries made of concentrated PC based electrolytes.^{38,49} The reduced co-intercalation of PC is attributed to the change in the solvation structure of Li⁺ ions.^{29,31,50} Molecular dynamics (MD) and quantum mechanics (QM) simulation studies played an important role in understanding the variation in the solvation structure of the ions and the dynamic behavior of the electrolyte with salt concentration, cation transport, and diffusion mechanisms within bulk electrolyte systems.^{51–56}

The conventional LIBs are found to operate optimally in the temperature range of $15\text{--}35^\circ\text{C}$ and typically operate at temperatures up to 60°C .^{57–59} However, it is to be noted that the fast charging and operation of LIBs result in generation of heat causing a significant rise in temperature,⁶⁰ which can affect the dynamic behavior and various properties of the electrolytes. The ionic conductivity of the electrolyte is significantly affected by the variations in temperature depending upon the age of the battery, especially at elevated temperatures.^{57,58,61} The impact of temperature on various properties of widely used 1M lithium electrolytes is well studied.^{54,62} However, such studies are limited for the electrolytes of higher concentration (e.g., $c \approx 3\text{M}$), which are now considered to be the candidate electrolytes for safer and durable LIBs and beyond lithium ion battery technologies.⁴⁵ The study of the effect of temperature on various properties of the concentrated electrolytes such as conductivity and viscosity helps one to tailor them to offer better performance over a range of temperatures and design thermal management systems such as active/passive cooling systems for battery packs. In the present work, we simulate the PC–LiPF₆ electrolyte of concentration $c = 3\text{ mol/kg}$ at various temperatures

ranging from $T = 298$ to 378 K using molecular dynamics (MD) simulations to study the bulk behavior of the electrolyte. We further compare and contrast the results with that of the dilute electrolyte of concentration, $c = 0.5\text{ mol/kg}$.

II. SIMULATION METHODOLOGY

Classical molecular dynamics simulations are carried out to study the temperature-altered behavior of the concentrated PC–LiPF₆ electrolyte. The inter- and intra-molecular interactions are modeled using the class II force field. The CFF93 parameters reported by Sun *et al.*⁶³ are used to enable the bonded interactions of the PC solvent. The parameters reported by Sharma and Ghorai⁶⁴ are used for the bonded interactions of PF₆[−] ions. The Lennard-Jones (LJ) parameters and partial atomic charges for PC and LiPF₆ are taken from the studies of Soetens, Millot, and Maigret,⁶⁵ Jorn *et al.*,⁶⁶ and Sharma and Ghorai,⁶⁴ respectively. Refer to Tables S1–S8 of the [supplementary material](#) for further details.

We simulate PC–LiPF₆ electrolytes of two different salt concentrations ($c = 0.5$ and 3 mol/kg) at various temperatures ranging from 298 to 378 K . The simulated systems consist of 196 PC solvent molecules. The electrolyte of concentration $c = 3\text{ mol/kg}$ consists of 60 salt molecules, and the electrolyte of concentration $c = 0.5\text{ mol/kg}$ consists of 10 salt molecules.⁵³ These molecules are packed randomly into a cubic box of size $40 \times 40 \times 40\text{ \AA}^3$ using PACKMOL.⁶⁷ Refer to Table S9 of the [supplementary material](#) for details of equilibrium density, molarity, and volume of the simulation boxes for the electrolytes at various temperatures.

Large-scale Atomic/Molecular Massively Parallel Simulator (LAMMPS)⁶⁸ is used to perform MD simulations. Short-range LJ interactions are truncated at 12 \AA . The geometric mixing rule is used to compute the parameters for the LJ interactions between two different atoms. Long-range electrostatic interactions are computed using the Particle–Particle Particle–Mesh (PPPM) method.⁶⁹ Periodic boundary conditions are applied along all three directions to mimic bulk solution. An integration time step of 1 fs is used.

First, each simulation system is energy minimized using the conjugate gradient algorithm. This is followed by equilibration in the NPT ensemble at a pressure of $p = 1\text{ atm}$ and a high temperature of $T = 398\text{ K}$ for 1 ns . After this, the systems are further equilibrated in NPT and NVT ensembles for 1 ns each at the desired temperature. The prescribed temperature and pressure of 1 atm are maintained using the Nosé–Hoover thermostat (time constant— 0.1 ps) and Nosé–Hoover barostat (time constant— 1 ps), respectively.^{70,71} The systems are finally simulated in the NVE ensemble for sufficiently long (i.e., at least 4 ns) such that the systems attain their equilibrium (see Fig. S2 of the [supplementary material](#)). We compare the radial distribution functions (RDFs) obtained from different time frames. The time invariance of RDFs is used as a criterion to verify the attainment of equilibrium. An electrolyte of $c = 3\text{ mol/kg}$ is run for a longer time for systems simulated at lower temperatures ($T = 298\text{ K}$ to $T = 328\text{ K}$) to achieve equilibration. The equilibrated systems are simulated for a production run of 50 ns in the case of $c = 0.5\text{ mol/kg}$ electrolytes and 60 ns for the electrolytes of $c = 3\text{ mol/kg}$. The equilibrated systems are also utilized to find the viscosity of various electrolytes using the periodic perturbation method.⁷² The trajectories of various atoms are recorded at every 1 ps during the production (NVE) run and

are post-processed to obtain various properties. The average values computed from at least five independent runs are presented in Sec. III.

III. RESULTS AND DISCUSSION

A. Transport properties

We analyze the transport properties of the electrolytes such as self-diffusivity of the ions, cationic transference number, and molar conductivity at various temperatures to understand the impact of temperature on the behavior of concentrated electrolytes.

1. Diffusivity

The self-diffusion coefficient D of an ion (or a molecule) can be computed from its mean-square displacement (MSD) using the Einstein relation,⁷³

$$D = \frac{1}{6} \lim_{t \rightarrow \infty} \frac{d}{dt} \langle [\mathbf{r}(t) - \mathbf{r}(0)]^2 \rangle, \quad (1)$$

where $\mathbf{r}(t)$ is position of the ion at time t and $\langle \rangle$ represents ensemble averaging of MSD. We fit a linear function to the MSD data in the long-time limit to obtain D . Refer to Figs. S3 and S4 of the [supplementary material](#) for further details.

In Fig. 1, we show the diffusivity of Li^+ and PF_6^- ions in the electrolyte of concentration $c = 3$ mol/kg at various temperatures (T) ranging from $T = 298$ K [i.e., $(1000/T) \approx 3.35$ K^{-1}] to 378 K [i.e., $(1000/T) \approx 2.65$ K^{-1}]. It is to be noted that D of PF_6^- shown in Fig. 1 is obtained from MSD of P (i.e., central atom of the PF_6^- ion).⁷⁴ Figure 1 also shows D of the ions in the dilute electrolyte of $c = 0.5$ mol/kg for the same temperature range. It shows good agreement with the literature.⁷⁵ In addition, the comparison data shown in Table S10 of the [supplementary material](#) suggests that the simulation systems considered are appropriate. At any given temperature, D of ions in the electrolyte of $c = 3$ mol/kg is

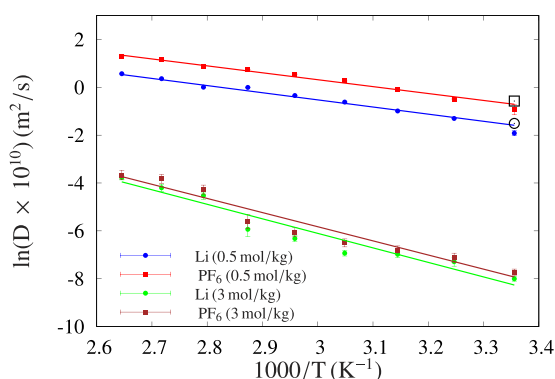


FIG. 1. Effect of temperature on diffusivity of ions. The diffusivity of Li^+ (circles) and PF_6^- (squares) ions is plotted as a function of $1000/T$ for electrolytes of salt concentrations $c = 0.5$ and 3 mol/kg. D of ions increases exponentially with increasing temperature. The solid lines show the Arrhenius fits [i.e., Eq. (2)] to the data. The open symbols (D_{Li} —circle and D_{PF_6} —square) denote the values simulated in the literature for $c = 0.569$ M by Takeuchi *et al.*⁷⁵

TABLE I. Arrhenius activation energy E_a (kcal/mol) for Li^+ and PF_6^- ions for systems described in Fig. 1.

Salt concentration (mol/kg)	Li^+	PF_6^-
0.5	5.82	5.74
3.0	12.07	11.74

lower (about 100 times at high temperatures) compared to that of the dilute electrolyte. The reduction in ion diffusivities at higher concentration can be attributed to the higher viscosity of the concentrated electrolytes (see Fig. 3), which hinders the diffusive motion of ions.⁷⁶

As shown in Fig. 1, the temperature significantly impacts the diffusivity of both the ions, independent of the concentration of the electrolyte. We also observe that for both concentrations, diffusivity increases exponentially with temperature, which can be approximated using the Arrhenius relation,

$$\ln D(T) = \ln D_\infty - \frac{E_a}{k_B T}, \quad (2)$$

where D_∞ is the limiting value of D , E_a is the activation energy, and k_B is the Boltzmann constant. Equation (2) suggests that the increase in temperature or decrease in E_a results in faster diffusion. We calculate E_a for both the ions by fitting the data presented in Fig. 1 to Eq. (2). The resulting values are reported in Table I. For a given concentration, E_a is nearly the same for both the ions. However, a change in concentration from $c = 0.5$ to 3 mol/kg leads to approximate doubling of the activation energy. It means that the ionic diffusivity in concentrated electrolytes shows stronger dependence on temperature compared to that of the dilute electrolytes. It indicates that transport properties are more sensitive to temperature for the batteries made of concentrated electrolytes.

Higher E_a values observed for the 3 mol/kg electrolyte indicate the higher energy barrier for the ions to diffuse through the surrounding fluid medium. It suggests that the molecular arrangement of the concentrated electrolyte is not as conducive as that of the dilute electrolyte for the ions to diffuse. It can be attributed to strong Coulombic interactions between the ions (due to the lack of sufficient solvent molecules to screen the charge), resulting in the formation of associated salt complexes at a higher concentration (see Fig. 5).⁷⁷

2. Transference number

The cation transference number describes the fraction of total current transported due to the migration of Li^+ ions (i.e., cation). The low cation transference number indicates the lower mobility of the cation compared to that of the anion. When subjected to high currents, electrolytes with a low cation transference number are susceptible to large concentration gradients. Conversely, the high transference number allows batteries to operate at large constant currents and achieve high charging rates, while mitigating internal resistance and extending their efficiency.^{78,79}

In MD simulations, one can compute the apparent cation transference number (t^+) from ion diffusivities as

TABLE II. Apparent cationic transference numbers (t^+) with absolute errors as a function of temperature for electrolytes of concentrations $c = 0.5$ and 3 mol/kg.

Temp. (K)	t^+ (0.5 mol/kg)	t^+ (3 mol/kg)
298	0.27 ± 0.003	0.43 ± 0.021
308	0.31 ± 0.003	0.45 ± 0.014
318	0.29 ± 0.010	0.46 ± 0.023
328	0.29 ± 0.008	0.40 ± 0.010
338	0.29 ± 0.004	0.43 ± 0.011
348	0.31 ± 0.011	0.42 ± 0.028
358	0.31 ± 0.009	0.46 ± 0.022
368	0.30 ± 0.007	0.40 ± 0.018
378	0.32 ± 0.018	0.45 ± 0.044

$$t^+ = \frac{D_{\text{Li}}}{D_{\text{Li}} + D_{\text{PF}_6}}. \quad (3)$$

Table II shows the comparison of t^+ for electrolytes of $c = 0.5$ and $c = 3$ mol/kg at various temperatures. The electrolytes do not show any noticeable dependency of t^+ on temperature. It indicates an identical impact of temperature on the diffusivity of both the ions (i.e., the change in D of both the ions with temperature is proportional). On the contrary, we observe the significant influence of salt concentration on t^+ . The t^+ values of the electrolyte of $c = 0.5$ mol/kg are lower than the values of the electrolyte of $c = 3$ mol/kg. The reduced difference between D_{Li} and D_{PF_6} for the $c = 3$ mol/kg electrolyte (Fig. 1) reflects in increased t^+ . The observed lower Li^+ ion diffusivity (clearly seen in the case of electrolyte of $c = 0.5$ mol/kg) can be attributed to the bulky and tightly coordinated Li^+ -PC complex (i.e., tight solvation shell of Li^+).^{80,81} Refer to Fig. S12 of the [supplementary material](#) for further details. For the electrolytes of higher concentration, the reduced availability of solvent molecules per Li^+ ion makes the first coordination shell of Li^+ less bulky compared to the same in a dilute electrolyte.⁸² In turn, it leads to a reduced difference between the diffusivities of the ions. Thus, the higher transference number observed for the concentrated electrolytes in Table II and the significant presence of associated ionic complexes in the 3 mol/kg electrolytes (see Fig. 5) suggest the correlated (associated) motion of Li^+ and PF_6^- ions in the concentrated electrolytes.^{77,83}

3. Molar conductivity

The conductivity of an electrolyte is a measure of its ability to conduct electricity. In this study, we compute the molar conductivity (Λ) of the electrolyte by using the collective displacement of ions as⁸⁴

$$\Lambda = \frac{N_A e^2}{6n k_B T} \lim_{t \rightarrow \infty} \frac{d}{dt} \sum_i \sum_j z_i z_j \langle \Delta \mathbf{r}_i \cdot \Delta \mathbf{r}_j \rangle, \quad (4)$$

where N_A is the Avogadro number, e is an electron charge, n is the number of ions, z_i is the charge on ion i , and $\Delta \mathbf{r}_i = \mathbf{r}_i(t) - \mathbf{r}_i(0)$ is the displacement of ion i . Refer to Fig. S5 of the [supplementary material](#) for further details.

In Fig. 2, we show the molar conductivities of electrolytes of concentrations 3 and 0.5 mol/kg for a range of temperatures. As the

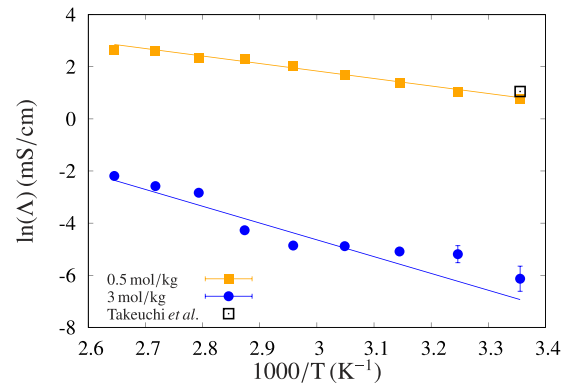


FIG. 2. Effect of temperature on the molar conductivity (Λ) of electrolytes. Λ is plotted as a function of $1000/T$ for electrolytes of salt concentrations $c = 0.5$ mol/kg (squares) and 3 mol/kg (circles). Λ increases exponentially with temperature for both the electrolytes. The solid lines show the Arrhenius (exponential) fits to the data. The open symbol denotes the simulated Λ data from the literature for $c = 0.569\text{M}$ by Takeuchi *et al.*⁷⁵

temperature increases, the conductivity of the electrolytes increases in an exponential manner. As expected, the variation in conductivity with temperature is high for the concentrated electrolyte compared to that of the dilute electrolyte. However, the magnitude of molar conductivity for the $c = 3$ mol/kg electrolyte is significantly smaller. The molar conductivity can be impacted by both the association of the salt ions and the bulk property of the electrolyte such as viscosity.

4. Viscosity

We compute the viscosity η of the electrolytes using the non-equilibrium periodic-perturbation method described by Hess.⁷² In this method, the response of an electrolyte (at equilibrium) to a set of applied periodic forces is studied to find its viscosity. We apply a unidirectional external force (i.e., x-component force), defined by the acceleration,

$$\begin{aligned} a_x(z) &= A \cos\left(\frac{2\pi z}{l_z}\right), \\ a_y(z) &= 0, \\ a_z(z) &= 0, \end{aligned} \quad (5)$$

to the atoms of the simulation box. Here, l_z is the length of the simulation box in the z -direction and A is the amplitude of the periodic acceleration in the z -direction: $a_x(z)$. The applied acceleration results in a velocity profile that is a function of only z within the simulation system,

$$u_x(z) = V \cos\left(\frac{2\pi z}{l_z}\right). \quad (6)$$

Here, V is the amplitude of the velocity. The steady-state Navier–Stokes equation for this system is given as

$$-\rho a_x(z) = \eta \frac{\partial^2 u_x(z)}{\partial z^2}, \quad (7)$$

where ρ is the density of electrolyte. The shear viscosity as a function of A is defined as⁷²

$$\eta(A) = \frac{A}{V} \frac{\rho}{\left(\frac{2\pi}{l_x}\right)^2}. \quad (8)$$

In the simulations conducted to find the viscosity of the electrolytes, we apply the acceleration of various amplitudes A within the range of 0.14 to 0.28 nm/ps² depending upon the salt concentration and the temperature of the electrolytes.^{85,86} The simulation runs of length 1 ns are carried out for each of the A values considered. Following Doherty and Acevedo,⁸⁵ we extrapolate the obtained $\eta(A)$ values to the $A = 0$ limit (see Fig. S6 of the [supplementary material](#) for further details) to obtain the viscosity.

As shown in [Fig. 3](#), the viscosity of both the electrolytes decreases linearly with the increase in temperature. It is expected that at high temperature the constituent particles of the electrolyte possess higher thermal energy, leading to frequent disruption of the molecular structure formed due to inter-molecular interactions. In turn, it leads to reduction in the viscosity of the electrolytes with temperature. We note that the degree of change in the viscosity of the concentrated electrolyte for unit change in temperature is high compared to that of the dilute electrolyte. It explains the higher impact of temperature on the diffusivity of ions in concentrated electrolytes shown in [Fig. 1](#). The observed behavior of the decrease in the viscosity of concentrated electrolytes (compared to dilute electrolytes) with the increase in temperature may emerge from the fact that at high temperature, the ion-solvent and salt complexes undergo frequent rearrangement due to involved thermal energy fluctuations (i.e., the frequency of formation and breakage of complexes is high at high temperature).⁸⁷ In [Sec. III B](#), we study structural properties and salt ion complexes of concentrated electrolytes to further understand the reasons for higher sensitivity of dynamic properties such as self-diffusivity of ions, molar conductivity, and viscosity to the temperature.

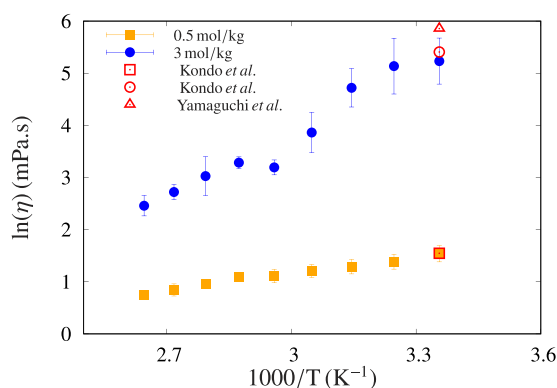


FIG. 3. Effect of temperature on the viscosity (η) of electrolytes. η in mPa s is plotted as a function of $1000/T$ for electrolytes of salt concentrations $c = 0.5$ mol/kg (squares) and 3 mol/kg (circles). η of both the electrolytes decreases with the increase in temperature. The open symbols denote the η values from the literature. Square: $c = 0.565$ M by Kondo *et al.*,⁸⁸ circle: $c = 2.91$ M by Kondo *et al.*,⁸⁸ and triangle: 3 mol/kg by Yamaguchi *et al.*⁸⁹ at 298 K.

B. Structural properties

Spatial distribution of ions and solvent molecules in the electrolyte (i.e., molecular arrangement in the electrolyte) can be quantified using the radial distribution functions (RDF).⁹⁰ The Li-O_c RDF describing how the PC molecules surround the Li⁺ ion is defined as

$$g_{\text{Li},\text{O}_c}(r) = \frac{n(r)}{4\pi\rho r^2 \Delta r}, \quad (9)$$

where O_c denotes the carbonyl oxygen atom of the PC molecule (see [Fig. S1](#) of the [supplementary material](#)), $n(r)$ is the number of O_c atoms present in a spherical shell of thickness Δr at a distance r from the position of the Li⁺ ion. Similarly, the relative arrangement of Li⁺ and PF₆⁻ ions in the electrolyte can be given by the RDF of Li-P ($g_{\text{Li},\text{P}}$) and Li-F ($g_{\text{Li},\text{F}}$) pairs.

[Figure 4](#) shows g_{Li,O_c} at various temperatures for the electrolyte of concentration $c = 3.0$ mol/kg. A sharp peak at $r \approx 1.8$ Å indicates a tight solvation shell. [Figure 4](#) also shows $g_{\text{Li},\text{F}}$ and $g_{\text{Li},\text{P}}$. The first peaks are found at $r \approx 1.65$ Å and $r \approx 3.15$ Å, respectively. The peak positions of g_{Li,O_c} , $g_{\text{Li},\text{F}}$, and $g_{\text{Li},\text{P}}$ compare well with the literature.^{65,75} A plot similar to [Fig. 4](#) for $c = 0.5$ mol/kg is shown in the [supplementary material](#) (see [Fig. S9](#)). The comparison of various RDFs in [Fig. 4](#) for a range of temperatures shows that there is little or no change in the position of peaks and their heights in the RDFs. It suggests that the change in temperature does not affect the relative distribution of solvent molecules and ions in the electrolyte.

The coordination number (CN) of O_c with respect to the Li⁺ ion is computed using the following equation:⁹¹

$$\text{CN}_{\text{Li},\text{O}_c} = \int_0^{r_{\text{min}}} g_{\text{Li},\text{O}_c}(r) dr. \quad (10)$$

Here, r_{min} refers to the first minima of g_{Li,O_c} , $r = 2.4$ Å. As shown in [Fig. S10](#) of the [supplementary material](#), Li⁺ ions have only three PC molecules on an average in the first coordination shell. However, for the electrolyte of $c = 0.5$ mol/kg, Li⁺ is coordinated by four

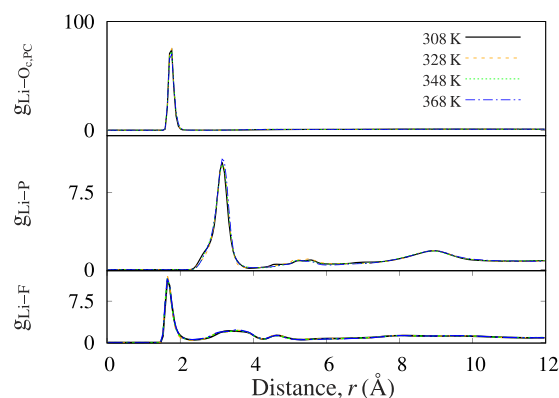


FIG. 4. Effect of temperature on the relative arrangement of molecules in the electrolyte of salt concentration $c = 3$ mol/kg. Radial distribution functions (RDFs) of Li-O_c (top row), Li-P (second row), and Li-F (bottom row) are presented for various temperatures.

PC molecules. The total coordination number of the Li^+ ion shell is 4, independent of the concentration and temperature. $\text{CN}_{\text{Li},\text{O}_c} = 3$ observed for concentrated electrolyte indicates that PF_6^- ions replace at least a PC molecule from the first coordination shell of the Li^+ ion. It also indicates a higher degree of association of the two oppositely charged ions in the concentrated electrolyte.

1. Salt-ion complexes

In an electrolyte of high concentration, ions have a tendency to associate and form complexes. The ionic complexes can be classified into contact ion pairs (CIPs) or aggregates (AGGs) depending upon the degree of ionic association. We use r_{\min} of $g_{\text{Li},\text{P}}(r) = 3.60 \text{ \AA}$ as a cutoff distance to identify the associated ions. An ion pair (i.e., Li^+ and PF_6^-) is said to be a CIP if only one counter ion is present in the spherical shell of a given Li^+ ion. The ionic complex is said to be an aggregate (AGG) when a counter ion present within the cutoff distance from the center of the Li^+ ion is paired with other Li^+ ions or when two or more number of counter ions are present within the cutoff distance. The Li^+ ions having no counter ion present in the spherical shell of the radius r_{\min} are considered as free ions or solvent separated ion pairs (SSIPs).

In the electrolyte of 3 mol/kg salt concentration, ions form a range of complexes. In Fig. 5, we show the percentage of Li^+ present in the form of various complexes for a range of temperatures. As seen, the associated ionic complexes are, in general, found more than SSIPs and the temperature does not show a significant impact on the nature of complexes as well. The presence of aggregates at $c = 3 \text{ mol/kg}$ explains the reduced difference in the diffusivities of Li^+ and PF_6^- ions (Fig. 1) and higher cationic transference numbers (Table II). In Sec. III B 2, we analyze the dynamic behavior of these ionic complexes to understand the effect of temperature.

2. Interaction dynamics

The mean residence time t_r of the PF_6^- ion forming a complex with the Li^+ ion helps us in determining the kinetics of the formation

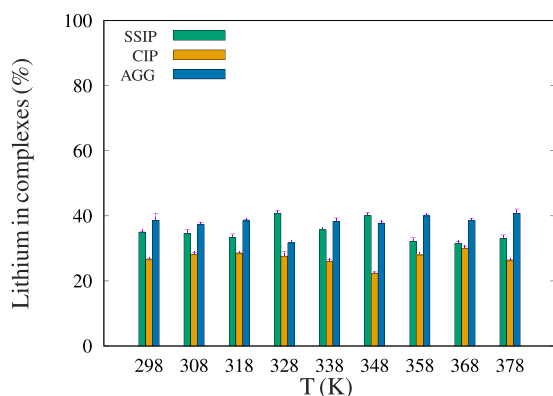


FIG. 5. Effect of temperature on the complexation of ions for electrolytes of salt concentration $c = 3 \text{ mol/kg}$. Percentages of lithium existing as various salt complexes: Solvent separated ion pairs (SSIPs), contact-ion pairs (CIPs), and aggregates (AGGs) are presented for temperatures ranging from $T = 298$ to 378 K .

of ionic complexes such as CIPs and aggregates. It is computed using the residence correlation function given by

$$C(t) = \frac{\langle H(t)H(0) \rangle}{\langle H(0)H(0) \rangle}, \quad (11)$$

where H denotes the Heaviside function.⁹² If the PF_6^- ion is present inside the sphere of radius, r_c centered at the Li^+ ion, $H(t) = 1$, otherwise $H(t) = 0$. We consider r_{\min} of $g_{\text{Li},\text{P}}(r)$ as the cutoff radius, r_c . The $H(t)$ data of various $\text{Li}-\text{P}$ pairs at time intervals of 2 ps are considered to compute $C(t)$ using Eq. (11). We express the $C(t)$ data as a series of six exponential functions,

$$C(t) = \sum_i a_i e^{-b_i t}, \quad (12)$$

and compute t_r by analytically integrating the series [Eq. (12)] as

$$t_r = \int_0^\infty C(t) dt. \quad (13)$$

The upper limit of integration is considered as high as 10^9 fs (see Fig. S7 of the supplementary material). The computed t_r values for different temperatures are reported in Fig. 6. With increasing temperature, we observe an exponential decay in t_r values. This implies that the thermal energy acquired by the ions affects the lifetime of the CIPs and AGGs.

A similar exercise is conducted to study the interaction time of the solvent molecules in the first coordination shell of Li^+ ions. The distance between the Li^+ ion and O_c atom of the PC molecule is used to compute the t_r values for Li^+-PC pairs.^{53,84,93} Here, r_c used for the evaluation of $C(t)$ in Eq. (11) is assumed to be r_{\min} of $g_{\text{Li},\text{O}_c}(r) = 2.4 \text{ \AA}$. Figure 6 shows a drop in the t_r values of the $\text{Li}-\text{O}_c$ pair with an increase in temperature. The comparison of the t_r values of

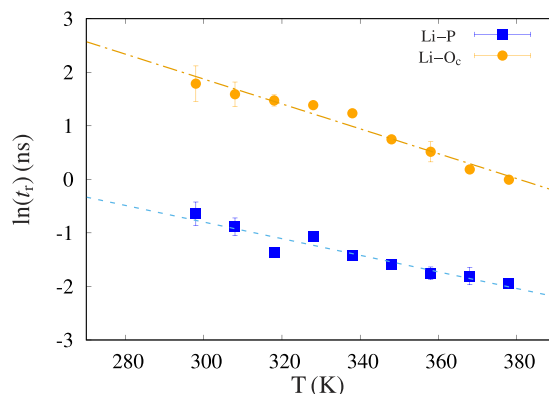


FIG. 6. Effect of temperature on the residence times (t_r) of PC molecules and PF_6^- ions in the first coordination shell of the Li^+ ion for electrolytes of salt concentration $c = 3 \text{ mol/kg}$. As the temperature increases, t_r of both PC and PF_6^- decay exponentially. The straight lines depict the exponential fits to the data.

Li-O_c and Li-P suggests that the Li⁺-PF₆⁻ ionic complex structures are more dynamic in nature than the Li⁺-PC solvation structures. We fit an exponential function $t_r = \alpha e^{-\beta T}$ to t_r vs temperature data. Though the decay factor to Li-P data ($\beta = 0.03$ ns/K) is not significantly different from that of the fit to Li-O_c data (0.05 ns/K), the higher β value for Li-O_c suggests that the thermal energy assists in the rupturing of Li⁺ solvation structures more than that of Li⁺-PF₆⁻ ionic complexes.

Temperature plays a significant role in altering the transport properties of the concentrated electrolytes. The diffusivity and conductivity of the electrolyte show an exponential increase with temperature. This can be partly attributed to the decrease in viscosity of the electrolyte with the increase in temperature. The analysis of the molecular structure of the electrolyte in terms of radial distribution functions and ion-complex classification suggest that the change in temperature does not affect the arrangement of the molecules in the electrolyte notably. The residence time analysis of ionic and salt-solvent complexes suggests that temperature significantly impacts the dynamic behavior of the complexes. The higher thermal energy associated with molecules of the electrolyte at high temperature results in faster dynamics, i.e., faster exchange of counter ions and solvent molecules from the first coordination shell of lithium ions. Consequently, the temperature plays a crucial role in defining the electrolyte behavior that may impact the overall battery performance with temperature variations.

IV. CONCLUSION

Molecular dynamics simulations of LiPF₆ in the PC electrolyte of concentration $c = 3$ mol/kg are conducted for a range of temperatures $T = 298$ – 378 K to understand the effect of temperature on various properties of the concentrated electrolyte. It shows that the temperature impacts transport properties such as diffusivity of ions, molar conductivity, and viscosity of the electrolytes. We further compare these properties with those of the dilute electrolyte of concentration $c = 0.5$ mol/kg. For all the temperatures studied, the ionic diffusivities and molar conductivities of concentrated electrolytes are significantly lower. It also shows that the transport properties of the concentrated electrolytes are more sensitive to the temperature variation. It can be attributed to strong Coulombic interactions between the ions due to the lack of sufficient solvent molecules to screen the charge on the ions, which in turn results in the formation of ionic complexes.

Concentrated electrolytes show the formation of a significant fraction of contact-ion pairs and aggregates. However, temperature has no or marginal effect on the structural properties of the electrolytes. The residence time analysis suggests that the interaction times of both the Li⁺-PF₆⁻ and Li⁺-PC pairs decrease with the increase in temperature. The observations made in the present study show that the transport properties and dynamic behavior of concentrated electrolytes are more sensitive to temperature compared to the dilute electrolytes, which asks for better thermal management of the batteries made with the former class of electrolytes. To reap the benefits offered by the concentrated electrolytes that are proposed to be the candidate electrolytes for advanced lithium ion batteries, one needs to carefully account for the

impact of the operating range of temperatures of the battery on the performance of the electrolytes.

SUPPLEMENTARY MATERIAL

See the [supplementary material](#) file for the force-field equation and the parameters, comparison of the properties of pure PC with the experimental values, effect of temperature on the box volume, density, and molarity of the electrolyte, description on the computation of transport and dynamic properties (D , Λ , η , t_r) and sample figures explaining the methodology, system size study of the transport properties, RDF of Li⁺-O_c, Li⁺-P and Li⁺-F RDF for the electrolyte of concentration $c = 0.5$ mol/kg, RDF and CN of P-O_c for both the concentrations, and potential of the mean force (PMF) comparison of Li⁺-PC and PF₆⁻-PC at $c = 0.5$ mol/kg.

DATA AVAILABILITY

The data that support the findings of this study are available from the corresponding author upon reasonable request.

REFERENCES

- 1 G. Martin, L. Rentsch, M. Höck, and M. Bertau, "Lithium market research—global supply, future demand and price development," *Energy Storage Mater.* **6**, 171–179 (2017).
- 2 G. Berdichevsky, K. Kelty, J. Straubel, and E. Toomre, "The tesla roadster battery system," *Tesla Motors* **1**, 1–5 (2006).
- 3 A. Opitz, P. Badami, L. Shen, K. Vignarooban, and A. M. Kannan, "Can Li-ion batteries be the panacea for automotive applications?," *Renewable Sustainable Energy Rev.* **68**, 685–692 (2017).
- 4 W. Jung, J. Jeong, J. Kim, and D. Chang, "Optimization of hybrid off-grid system consisting of renewables and Li-ion batteries," *J. Power Sources* **451**, 227754 (2020).
- 5 A. Lebkowski, "Temperature, overcharge and short-circuit studies of batteries used in electric vehicles," *Przegl. Elektrotech.* **1**, 69–75 (2017).
- 6 X. Feng, C. Weng, M. Ouyang, and J. Sun, "Online internal short circuit detection for a large format lithium ion battery," *Appl. Energy* **161**, 168–180 (2016).
- 7 F. Larsson, P. Andersson, P. Blomqvist, A. Lorén, and B.-E. Mellander, "Characteristics of lithium-ion batteries during fire tests," *J. Power Sources* **271**, 414–420 (2014).
- 8 F. Larsson, P. Andersson, P. Blomqvist, and B.-E. Mellander, "Toxic fluoride gas emissions from lithium-ion battery fires," *Sci. Rep.* **7**, 10018 (2017).
- 9 J. Ye, H. Chen, Q. Wang, P. Huang, J. Sun, and S. Lo, "Thermal behavior and failure mechanism of lithium ion cells during overcharge under adiabatic conditions," *Appl. Energy* **182**, 464–474 (2016).
- 10 Q. Yuan, F. Zhao, W. Wang, Y. Zhao, Z. Liang, and D. Yan, "Overcharge failure investigation of lithium-ion batteries," *Electrochim. Acta* **178**, 682–688 (2015).
- 11 Q. Wang, P. Ping, X. Zhao, G. Chu, J. Sun, and C. Chen, "Thermal runaway caused fire and explosion of lithium ion battery," *J. Power Sources* **208**, 210–224 (2012).
- 12 S. Hess, M. Wohlfahrt-Mehrens, and M. Wachtler, "Flammability of Li-ion battery electrolytes: Flash point and self-extinguishing time measurements," *J. Electrochem. Soc.* **162**, A3084 (2015).
- 13 E. P. Roth and C. J. Orendorff, "How electrolytes influence battery safety," *Electrochem. Soc. Interface* **21**, 45 (2012).
- 14 N. Ehteshami, L. Ibing, L. Stolz, M. Winter, and E. Paillard, "Ethylene carbonate-free electrolytes for Li-ion battery: Study of the solid electrolyte interphases formed on graphite anodes," *J. Power Sources* **451**, 227804 (2020).

- ¹⁵S. Gantenbein, M. Schönleber, M. Weiss, and E. Ivers-Tiffée, “Capacity fade in lithium-ion batteries and cyclic aging over various state-of-charge ranges,” *Sustainability* **11**, 6697 (2019).
- ¹⁶N. Saqib, C. M. Ganim, A. E. Shelton, and J. M. Porter, “On the decomposition of carbonate-based lithium-ion battery electrolytes studied using operando infrared spectroscopy,” *J. Electrochem. Soc.* **165**, A4051 (2018).
- ¹⁷S. S. Zhang, T. R. Jow, K. Amine, and G. L. Henriksen, “LiPF₆-EC-EMC electrolyte for Li-ion battery,” *J. Power Sources* **107**, 18–23 (2002).
- ¹⁸K. Tikhonov and V. Koch, “Li-ion battery electrolytes designed for a wide temperature range,” Technical Report No. ADA507154, Covalent Associates, Inc., Woburn, MA, 2006.
- ¹⁹J.-S. Kim, M.-S. Paik, J.-J. Park, Y.-G. Kim, J.-S. Kim, H.-S. Kim, S.-j. Lee, J.-H. Nah, S.-M. Hwang, C.-J. Kim *et al.*, “Electrolyte for lithium secondary battery and lithium secondary battery comprising same,” US patent 7,241,536 (10 July 2007).
- ²⁰C. L. Berhaut, D. Lemordant, P. Porion, L. Timperman, G. Schmidt, and M. Anouti, “Ionic association analysis of LiTfDI, LiFSI and LiPF₆ in EC/DMC for better Li-ion battery performances,” *RSC Adv.* **9**, 4599–4608 (2019).
- ²¹S. Uchida and T. Kiyobayashi, “How does the solvent composition influence the transport properties of electrolyte solutions?—LiPF₆ and LiFSA in EC and DMC binary solvent,” *Phys. Chem. Chem. Phys.* **23**, 10875–10887 (2021).
- ²²M. Watanabe, M. L. Thomas, S. Zhang, K. Ueno, T. Yasuda, and K. Dokko, “Application of ionic liquids to energy storage and conversion materials and devices,” *Chem. Rev.* **117**, 7190–7239 (2017).
- ²³C. Sun, J. Liu, Y. Gong, D. P. Wilkinson, and J. Zhang, “Recent advances in all-solid-state rechargeable lithium batteries,” *Nano Energy* **33**, 363–386 (2017).
- ²⁴L. Long, S. Wang, M. Xiao, and Y. Meng, “Polymer electrolytes for lithium polymer batteries,” *J. Mater. Chem. A* **4**, 10038–10069 (2016).
- ²⁵A. Eftekhari, “High-energy aqueous lithium batteries,” *Adv. Energy Mater.* **8**, 1801156 (2018).
- ²⁶Y. Yamada, J. Wang, S. Ko, E. Watanabe, and A. Yamada, “Advances and issues in developing salt-concentrated battery electrolytes,” *Nat. Energy* **4**, 269–280 (2019).
- ²⁷W. Dai, N. Dong, Y. Xia, S. Chen, H. Luo, Y. Liu, and Z. Liu, “Localized concentrated high-concentration electrolyte enhanced stability and safety for high voltage Li-ion batteries,” *Electrochim. Acta* **320**, 134633 (2019).
- ²⁸R. Petibon, C. P. Aiken, L. Ma, D. Xiong, and J. R. Dahn, “The use of ethyl acetate as a sole solvent in highly concentrated electrolyte for Li-ion batteries,” *Electrochim. Acta* **154**, 287–293 (2015).
- ²⁹O. A. Drozhzhin, V. A. Shevchenko, M. V. Zakharkin, P. I. Gamzyukov, L. V. Yashina, A. M. Abakumov, K. J. Stevenson, and E. V. Antipov, “Improving salt-to-solvent ratio to enable high-voltage electrolyte stability for advanced Li-ion batteries,” *Electrochim. Acta* **263**, 127–133 (2018).
- ³⁰D. W. McOwen, D. M. Seo, O. Borodin, J. Vatamanu, P. D. Boyle, and W. A. Henderson, “Concentrated electrolytes: Decoding electrolyte properties and reassessing Al corrosion mechanisms,” *Energy Environ. Sci.* **7**, 416–426 (2014).
- ³¹J. Wang, Y. Yamada, K. Sodeyama, C. H. Chiang, Y. Tateyama, and A. Yamada, “Superconcentrated electrolytes for a high-voltage lithium-ion battery,” *Nat. Commun.* **7**, 12032 (2016).
- ³²Y. Yamada, K. Furukawa, K. Sodeyama, K. Kikuchi, M. Yaegashi, Y. Tateyama, and A. Yamada, “Unusual stability of acetonitrile-based superconcentrated electrolytes for fast-charging lithium-ion batteries,” *J. Am. Chem. Soc.* **136**, 5039–5046 (2014).
- ³³L. Suo, W. Xue, M. Gobet, S. G. Greenbaum, C. Wang, Y. Chen, W. Yang, Y. Li, and J. Li, “Fluorine-donating electrolytes enable highly reversible 5-V-class Li metal batteries,” *Proc. Natl. Acad. Sci. U. S. A.* **115**, 1156–1161 (2018).
- ³⁴X. Fan, L. Chen, X. Ji, T. Deng, S. Hou, J. Chen, J. Zheng, F. Wang, J. Jiang, K. Xu, and C. Wang, “Highly fluorinated interphases enable high-voltage Li-metal batteries,” *Chem* **4**, 174–185 (2018).
- ³⁵J. Qian, W. A. Henderson, W. Xu, P. Bhattacharya, M. Engelhard, O. Borodin, and J.-G. Zhang, “High rate and stable cycling of lithium metal anode,” *Nat. Commun.* **6**, 6362 (2015).
- ³⁶S.-K. Jeong, M. Inaba, Y. Iriyama, T. Abe, and Z. Ogumi, “Electrochemical intercalation of lithium ion within graphite from propylene carbonate solutions,” *Electrochem. Solid-State Lett.* **6**, A13 (2002).
- ³⁷S.-K. Jeong, H.-Y. Seo, D.-H. Kim, H.-K. Han, J.-G. Kim, Y. B. Lee, Y. Iriyama, T. Abe, and Z. Ogumi, “Suppression of dendritic lithium formation by using concentrated electrolyte solutions,” *Electrochem. Commun.* **10**, 635–638 (2008).
- ³⁸M. Nie, D. P. Abraham, D. M. Seo, Y. Chen, A. Bose, and B. L. Lucht, “Role of solution structure in solid electrolyte interphase formation on graphite with LiPF₆ in propylene carbonate,” *J. Phys. Chem. C* **117**, 25381–25389 (2013).
- ³⁹K. Matsumoto, K. Inoue, K. Nakahara, R. Yuge, T. Noguchi, and K. Utsugi, “Suppression of aluminum corrosion by using high concentration LiTFSI electrolyte,” *J. Power Sources* **231**, 234–238 (2013).
- ⁴⁰S.-J. Cho, D.-E. Yu, T. P. Pollard, H. Moon, M. Jang, O. Borodin, and S.-Y. Lee, “Nonflammable lithium metal full cells with ultra-high energy density based on coordinated carbonate electrolytes,” *iScience* **23**, 100844 (2020).
- ⁴¹V. Nilsson, D. Bernin, D. Brandell, K. Edström, and P. Johansson, “Interactions and transport in highly concentrated LiTFSI-based electrolytes,” *ChemPhysChem* **21**, 1166–1176 (2020).
- ⁴²G. Chen, F. Zhang, Z. Zhou, J. Li, and Y. Tang, “A flexible dual-ion battery based on PVDF-HFP-modified gel polymer electrolyte with excellent cycling performance and superior rate capability,” *Adv. Energy Mater.* **8**, 1801219 (2018).
- ⁴³S.-K. Jeong, M. Inaba, Y. Iriyama, T. Abe, and Z. Ogumi, “Interfacial reactions between graphite electrodes and propylene carbonate-based solutions: Electrolyte-concentration dependence of electrochemical lithium intercalation reaction,” *J. Power Sources* **175**, 540–546 (2008).
- ⁴⁴K. Tasaki, A. Goldberg, J.-J. Liang, and M. Winter, “New insight into differences in cycling behaviors of a lithium-ion battery cell between the ethylene carbonate- and propylene carbonate-based electrolytes,” *ECS Trans.* **33**, 59–69 (2011).
- ⁴⁵S. Ko, Y. Yamada, and A. Yamada, “A 4.8 V reversible Li₂CoPo₄F/graphite battery enabled by concentrated electrolytes and optimized cell design,” *Batteries Supercaps* **3**, 910–916 (2020).
- ⁴⁶R. Naejus, D. Lemordant, R. Coudert, and P. Willmann, “Excess thermodynamic properties of binary mixtures containing linear or cyclic carbonates as solvents at the temperatures 298.15 K and 315.15 K,” *J. Chem. Thermodyn.* **29**, 1503–1515 (1997).
- ⁴⁷L. Xing, X. Zheng, M. Schroeder, J. Alvarado, A. von Wald Cresce, K. Xu, Q. Li, and W. Li, “Deciphering the ethylene carbonate-propylene carbonate mystery in Li-ion batteries,” *Acc. Chem. Res.* **51**, 282–289 (2018).
- ⁴⁸B. Ravikumar, M. Mynam, and B. Rai, “Molecular dynamics investigation of electric field altered behavior of lithium ion battery electrolytes,” *J. Mol. Liq.* **300**, 112252 (2020).
- ⁴⁹D. Zhu, H. Fan, and H. Wang, “PF₆-intercalation into graphite electrode from propylene carbonate,” *ACS Appl. Energy Mater.* **4**, 2181–2189 (2021).
- ⁵⁰J. Zheng, J. A. Lochala, A. Kwok, Z. D. Deng, and J. Xiao, “Research progress towards understanding the unique interfaces between concentrated electrolytes and electrodes for energy storage applications,” *Adv. Sci.* **4**, 1700032 (2017).
- ⁵¹J. Self, K. D. Fong, and K. A. Persson, “Transport in superconcentrated LiPF₆ and LiBF₄/propylene carbonate electrolytes,” *ACS Energy Lett.* **4**, 2843–2849 (2019).
- ⁵²A. V. Karantanos, T. Ohba, and Q. Cai, “Diffusion of ions and solvent in propylene carbonate solutions for lithium-ion battery applications,” *J. Mol. Liq.* **320**, 114351 (2020).
- ⁵³M. Mynam, B. Ravikumar, and B. Rai, “Molecular dynamics study of propylene carbonate based concentrated electrolyte solutions for lithium ion batteries,” *J. Mol. Liq.* **278**, 97–104 (2019).
- ⁵⁴P. Ganesh, D.-e. Jiang, and P. R. C. Kent, “Accurate static and dynamic properties of liquid electrolytes for Li-ion batteries from ab initio molecular dynamics,” *J. Phys. Chem. B* **115**, 3085–3090 (2011).
- ⁵⁵M. T. Ong, O. Vernali, E. W. Draeger, A. C. T. van Duin, V. Lordi, and J. E. Pask, “Lithium ion solvation and diffusion in bulk organic electrolytes from first-principles and classical reactive molecular dynamics,” *J. Phys. Chem. B* **119**, 1535–1545 (2015).
- ⁵⁶W. Zhang and L. R. Pratt, “AIMD results for a concentrated solution of tetra-ethylammonium tetra-fluoroborate in propylene carbonate,” *ECS Trans.* **66**, 1 (2015).

- ⁵⁷F. Leng, C. M. Tan, and M. Pecht, "Effect of temperature on the aging rate of Li ion battery operating above room temperature," *Sci. Rep.* **5**, 12967 (2015).
- ⁵⁸S. Ma, M. Jiang, P. Tao, C. Song, J. Wu, J. Wang, T. Deng, and W. Shang, "Temperature effect and thermal impact in lithium-ion batteries: A review," *Prog. Nat. Sci.: Mater. Int.* **28**, 653–666 (2018).
- ⁵⁹W. Chang, C. Bommier, T. Fair, J. Yeung, S. Patil, and D. Steingart, "Understanding adverse effects of temperature shifts on Li-ion batteries: An operando acoustic study," *J. Electrochem. Soc.* **167**, 090503 (2020).
- ⁶⁰A. Tomaszewska, Z. Chu, X. Feng, S. O'Kane, X. Liu, J. Chen, C. Ji, E. Endler, R. Li, L. Liu *et al.*, "Lithium-ion battery fast charging: A review," *eTransportation* **1**, 100011 (2019).
- ⁶¹T. Waldmann, M. Wilka, M. Kasper, M. Fleischhammer, and M. Wohlfahrt-Mehrens, "Temperature dependent ageing mechanisms in lithium-ion batteries—A post-mortem study," *J. Power Sources* **262**, 129–135 (2014).
- ⁶²C. M. Tenney and R. T. Cygan, "Analysis of molecular clusters in simulations of lithium-ion battery electrolytes," *J. Phys. Chem. C* **117**, 24673–24684 (2013).
- ⁶³H. Sun, S. J. Mumby, J. R. Maple, and A. T. Hagler, "An ab initio CFF93 all-atom force field for polycarbonates," *J. Am. Chem. Soc.* **116**, 2978–2987 (1994).
- ⁶⁴A. Sharma and P. K. Ghorai, "Effect of water on structure and dynamics of [BMIM][PF₆] ionic liquid: An all-atom molecular dynamics simulation investigation," *J. Chem. Phys.* **144**, 114505 (2016).
- ⁶⁵J.-C. Soetens, C. Millot, and B. Maigret, "Molecular dynamics simulation of Li⁺ BF₄⁻ in ethylene carbonate, propylene carbonate, and dimethyl carbonate solvents," *J. Phys. Chem. A* **102**, 1055–1061 (1998).
- ⁶⁶R. Jorn, R. Kumar, D. P. Abraham, and G. A. Voth, "Atomistic modeling of the electrode–electrolyte interface in Li-ion energy storage systems: Electrolyte structuring," *J. Phys. Chem. C* **117**, 3747–3761 (2013).
- ⁶⁷L. Martínez, R. Andrade, E. G. Birgin, and J. M. Martínez, "PACKMOL: A package for building initial configurations for molecular dynamics simulations," *J. Comput. Chem.* **30**, 2157–2164 (2009).
- ⁶⁸S. Plimpton, "Fast parallel algorithms for short-range molecular dynamics," *J. Comput. Phys.* **117**, 1–19 (1995).
- ⁶⁹S. Plimpton, R. Pollock, and M. Stevens, "Particle-mesh Ewald and rRESPA for parallel molecular dynamics simulations," in *PPSC* (Citeseer, 1997).
- ⁷⁰S. Nosé, "A molecular dynamics method for simulations in the canonical ensemble," *Mol. Phys.* **52**, 255–268 (1984).
- ⁷¹W. G. Hoover, "Canonical dynamics: Equilibrium phase-space distributions," *Phys. Rev. A* **31**, 1695 (1985).
- ⁷²B. Hess, "Determining the shear viscosity of model liquids from molecular dynamics simulations," *J. Chem. Phys.* **116**, 209–217 (2002).
- ⁷³A. Einstein *et al.*, "On the motion of small particles suspended in liquids at rest required by the molecular-kinetic theory of heat," *Ann. Phys.* **17**, 208 (1905).
- ⁷⁴B. Ravikumar, M. Mynam, and B. Rai, "Effect of salt concentration on properties of lithium ion battery electrolytes: A molecular dynamics study," *J. Phys. Chem. C* **122**, 8173–8181 (2018).
- ⁷⁵M. Takeuchi, Y. Kameda, Y. Umebayashi, S. Ogawa, T. Sonoda, S.-i. Ishiguro, M. Fujita, and M. Sano, "Ion–ion interactions of LiPF₆ and LiBF₄ in propylene carbonate solutions," *J. Mol. Liq.* **148**, 99–108 (2009).
- ⁷⁶K. S. Han, J. Chen, R. Cao, N. N. Rajput, V. Murugesan, L. Shi, H. Pan, J.-G. Zhang, J. Liu, K. A. Persson, and K. T. Mueller, "Effects of anion mobility on electrochemical behaviors of lithium–sulfur batteries," *Chem. Mater.* **29**, 9023–9029 (2017).
- ⁷⁷C. Geng, D. Buchholz, G. T. Kim, D. V. Carvalho, H. Zhang, L. G. Chagas, and S. Passerini, "Influence of salt concentration on the properties of sodium-based electrolytes," *Small Methods* **3**, 1800208 (2019).
- ⁷⁸Y. Lu, M. Tikekar, R. Mohanty, K. Hendrickson, L. Ma, and L. A. Archer, "Stable cycling of lithium metal batteries using high transference number electrolytes," *Adv. Energy Mater.* **5**, 1402073 (2015).
- ⁷⁹K. M. Diederichsen, E. J. McShane, and B. D. McCloskey, "Promising routes to a high Li⁺ transference number electrolyte for lithium ion batteries," *ACS Energy Lett.* **2**, 2563–2575 (2017).
- ⁸⁰A. V. Cresce, S. M. Russell, O. Borodin, J. A. Allen, M. A. Schroeder, M. Dai, J. Peng, M. P. Gobet, S. G. Greenbaum, R. E. Rogers, and K. Xu, "Solvation behavior of carbonate-based electrolytes in sodium ion batteries," *Phys. Chem. Chem. Phys.* **19**, 574–586 (2017).
- ⁸¹E. Flores, G. Åvall, S. Jeschke, and P. Johansson, "Solvation structure in dilute to highly concentrated electrolytes for lithium-ion and sodium-ion batteries," *Electrochim. Acta* **233**, 134–141 (2017).
- ⁸²L. Suo, Y.-S. Hu, H. Li, M. Armand, and L. Chen, "A new class of solvent-in-salt electrolyte for high-energy rechargeable metallic lithium batteries," *Nat. Commun.* **4**, 1481 (2013).
- ⁸³Y. Shao, M. Hellström, A. Yllö, J. Mindemark, K. Hermansson, J. Behler, and C. Zhang, "Temperature effects on the ionic conductivity in concentrated alkaline electrolyte solutions," *Phys. Chem. Chem. Phys.* **22**, 10426–10430 (2020).
- ⁸⁴O. Borodin and G. D. Smith, "Quantum chemistry and molecular dynamics simulation study of dimethyl carbonate: Ethylene carbonate electrolytes doped with LiPF₆," *J. Phys. Chem. B* **113**, 1763–1776 (2009).
- ⁸⁵B. Doherty and O. Acevedo, "OPLS force field for choline chloride-based deep eutectic solvents," *J. Phys. Chem. B* **122**, 9982–9993 (2018).
- ⁸⁶K. Nieszporek, J. Nieszporek, and M. Trojak, "Calculations of shear viscosity, electric conductivity and diffusion coefficients of aqueous sodium perchlorate solutions from molecular dynamics simulations," *Comput. Theor. Chem.* **1090**, 52–57 (2016).
- ⁸⁷S. Amara, J. Toulc'Hoat, L. Timperman, A. Biller, H. Galiano, C. Marcel, M. Ledigabel, and M. Anouti, "Comparative study of alkali-cation-based (Li⁺, Na⁺, K⁺) electrolytes in acetonitrile and alkylcarbonates," *ChemPhysChem* **20**, 581–594 (2019).
- ⁸⁸K. Kondo, M. Sano, A. Hiwara, T. Omi, M. Fujita, A. Kuwae, M. Iida, K. Mogi, and H. Yokoyama, "Conductivity and solvation of Li⁺ ions of LiPF₆ in propylene carbonate solutions," *J. Phys. Chem. B* **104**, 5040–5044 (2000).
- ⁸⁹T. Yamaguchi, T. Yonezawa, K. Yoshida, T. Yamaguchi, M. Nagao, A. Faraone, and S. Seki, "Relationship between structural relaxation, shear viscosity, and ionic conduction of LiPF₆/propylene carbonate solutions," *J. Phys. Chem. B* **119**, 15675–15682 (2015).
- ⁹⁰D. Frenkel and B. Smit, *Understanding Molecular Simulation: From Algorithms to Applications* (Academic Press, Cambridge, MA, 1996).
- ⁹¹Y. Shim, "Computer simulation study of the solvation of lithium ions in ternary mixed carbonate electrolytes: Free energetics, dynamics, and ion transport," *Phys. Chem. Chem. Phys.* **20**, 28649–28657 (2018).
- ⁹²R. W. Impey, P. A. Madden, and I. R. McDonald, "Hydration and mobility of ions in solution," *J. Phys. Chem.* **87**, 5071–5083 (1983).
- ⁹³X. Deng, M. Y. Hu, X. Wei, W. Wang, Z. Chen, J. Liu, and J. Z. Hu, "Natural abundance ¹⁷O nuclear magnetic resonance and computational modeling studies of lithium based liquid electrolytes," *J. Power Sources* **285**, 146–155 (2015).